Spring 2020

Comparison of Household-Scale Rainwater Harvesting and Greywater Recycling Systems in Boston Through Spatial Optimization of Cost and Energy Savings

Shannon K. Stang
University of New Hampshire, Durham

COMPARISON OF HOUSEHOLD-SCALE RAINWATER HARVESTING AND GREYWATER RECYCLING SYSTEMS IN BOSTON THROUGH SPATIAL OPTIMIZATION OF COST AND ENERGY SAVINGS

BY

SHANNON K. STANG
B.S. in Environmental Engineering, University of New Hampshire, 2018

THESIS

Submitted to the University of New Hampshire
in Partial Fulfillment of
the Requirements for the Degree of

Master of Science
in
Civil & Environmental Engineering

May 2020

This thesis was examined and approved in partial fulfillment of the requirements for the degree of Master of Science in Civil & Environmental Engineering by:

Dr. Weiwei Mo
Thesis Director
Assistant Professor, Department of Civil & Environmental Engineering

Dr. Michael Palace
Associate Professor, Department of Earth Sciences – Joint Positions

Dr. Marek Petrik
Assistant Professor, Department of Computer Science

On November 22nd, 2019

Approval signatures are on file with the University of New Hampshire Graduate School.

TABLE OF CONTENTS

38

LIST OF FIGURES

ABSTRACT

Comparison of Household-Scale Rainwater Harvesting and Greywater Recycling Systems in Boston Through Spatial Optimization of Cost and Energy Savings

by

Shannon K. Stang
University of New Hampshire

Household decentralized water systems, including rainwater harvesting and greywater recycling, are often touted as a means to improve the sustainability and resiliency of centralized municipal systems. This research is focused on the spatial distribution of life cycle energy savings and consumer cost savings of adopting decentralized systems for individual households in the city of Boston. Using a Python model simulation, the optimal type and size of decentralized system for each household is selected based on the cost and energy comparison between the installation, operation, and maintenance of the new system and the process of treatment and delivery from the existing utility. The decentralized system selection is based on household characteristics such as distance from the centralized plants, number of tenants, and roof size. The distribution of households was mapped to analyze the spatial distribution of the effects of adopting a decentralized system. Greywater recycling systems largely returned cost and energy savings after 30 years, while rainwater harvesting systems resulted in losses.

1. Introduction

Around 90% of the US population currently relies on centralized water supply systems, which are often characterized as infrastructure with distribution networks that provide service to an entire city or region (Dieter et al. 2018). With the benefit of economies-of-scale, these centralized systems can supply sufficient quantities of easily accessed, high-quality potable water with a relatively low cost to the consumers (Hunter et al. 2010). Nevertheless, management of these systems has become increasingly challenging. In the US, many crucial water conveyance pipes were installed over 100 years ago, while the total expected lifespan of the pipes is generally between 75 and 100 years (ASCE, 2017). The country has fallen behind on repairing or replacing aged water systems. There are an estimated 240,000 water main breaks per year, resulting in losses of around six billion gallons of treated water per day (ASCE, 2017). An estimated investment of $250 billion over the next 30 years is needed to replace the aged water pipes and fixtures (AWWA, 2001). Additionally, the centralized water supply scheme can have high vulnerability and lack adaptability to the increasingly common natural (e.g., droughts and flooding) and manmade (e.g., terrorist attacks) threats. On the other hand, decentralized water supply systems have been developed and increasingly integrated within the centralized network. Decentralized or distributed systems are smaller-scale dispersed facilities that are located near or at the point of use (JFW, 2014). They can either function independently or remain connected to a centralized system (JFW, 2014). Rainwater harvesting (RWH) and greywater recycling (GWR) systems are currently the two most widely investigated/implemented decentralized water systems (Ángel et al. 2016). Decentralized systems are often touted as money- and energy-saving investments (Wang et al. 2015). However, poorly sized or sited systems can lead to an increased cost for the consumer and a net energy loss (Wang and Zimmerman 2015). A holistic understanding of how the decentralized water systems can be integrated on a city-scale to improve sustainability and resiliency is hence imperative.

Over the last decade, life cycle assessment (LCA) and life cycle cost assessment (LCCA) have been increasingly applied for assessing RWH and GWR systems, although much uncertainty still exists as whether the decentralized systems can result in positive cost or energy savings. Many of these studies adopted a case study approach that focused on specific building settings (e.g., (Morales-Pinzón et al. 2015; Wang and Zimmerman 2015)), but did not consider the influence of adoption patterns on a city scale. They commonly suggested that RWH or GWR systems with a higher service population or population density are more likely to achieve cost or energy savings (e.g., (Godskesen et al. 2011; Jeong et al. 2016; Memon et al. 2007; Newman, Dandy, and Maier 2015; Wanjiru and Xia 2017; Ward, Memon, and Butler 2012)). Only a few of these studies have considered the avoided treatment and pumping needs at the centralized plants as a result of the adoption. Of these that did consider the avoided treatment and pumping needs, findings vary significantly depending on the design of the decentralized systems and the system boundary that has been included in the analysis. None of these studies, however, considered the influence of household location within the context of the existing centralized network on the avoided pumping needs (e.g. (Angrill et al. 2012; Ghimire et al. 2014; Godskesen et al. 2011, 2013; Newman, Dandy, and Maier 2015; Ward, Memon, and Butler 2012)).

Very few studies have examined the influence of integrating decentralized water systems into the existing centralized networks on a city scale. Matteo et al. (2017) investigated the optimized spatial distribution of RWH system adoptions based upon supply volume, water quality improvement, and life cycle cost. They found integrating RWH systems into the centralized network can improve the reliability of the water supply, but there is a tradeoff between reliability and cost. Similarly, Penn et al. (2013) optimized the spatial distribution of homes with GWR systems in a neighborhood to minimize life cycle energy cost and wastewater outflow using hydrodynamic modeling. They found the optimal amount of greywater water usage was highly related to the spatial location of the households. This study, however, did not include a full life cycle assessment. Neither studies, however, investigated the optimized sizing of the decentralized systems. Kavvada et al. (2016), on the other hand, investigated the optimal size and locations of shared

decentralized water reuse systems in San Francisco, CA. Optimal distribution was based on life cycle cost, energy and greenhouse-gas emissions which were determined by home elevation, population density, and road network analysis. This study determined that savings were more sensitive to spatial determinants for decentralized systems than their size or scale. One recent study investigated the optimal integration of GWR and RWH systems at a regional scale based upon water volume and cost savings (Hargreaves et al., 2019). However, life cycle energy savings as well as the avoided treatment and pumping needs from the centralized plants were not investigated.

Most of the previous studies often investigate RWH and GWR systems separately, making their comparisons difficult. Ghisi, Rupp, and Triska (2014) applied RWH, GWR, and other potable water saving methods to a single school building in Brazil to examine the energy and cost outcomes. The RWH system was found to have a shorter payback period compared with the GWR system. However, the study used fixed flow rates and sizes to model the systems over the systems' life span. On the other hand, Chang, Lee, and Yoon (2017) looked at the operation phases of GWR, RWH, as well as a typical centralized plant in South Korea to compare their energy consumptions. The GWR system was determined to be superior than both the RWH and the centralized water supply primarily due to the reduced amount of wastewater that needs to be treated. The completely different recommendations provided by the two studies are likely a result of the varied climate, building, and system settings that have been considered. This suggests the importance of developing models that can be easily generalized for different decentralized system applications.

Our study combines LCA and LCCA with system dynamics modeling, tank size optimization, and spatial analysis. This model gives individual households of varying sizes and characteristics an optimally sized greywater or rainwater system based upon its life cycle cost and energy expenditure. RWH and GWR systems were selected for this study due to their common household applications for onsite non-potable collection and reuse. Areas in a city that can benefit most from decentralized system integration were then

investigated. Boston, MA was selected as a study site given its expected population growth and aged water and wastewater infrastructure (Bowen et al. 2019). Our model aims to provide communities a tool that informs them of the feasibility of adopting decentralized systems based on energy and costs as well as to determine viable ways to efficiently conserve energy and dependably supply water to assist decision-making in water management policy.

2. Methodology

2.1 RWH and GWR System Description

Figure 1 illustrates the process of the modeling effort conducted in this study. Two system dynamics models, one for RWH and one for GWR, were first developed to simulate the daily water balance based upon the supply of rainwater or greywater, the non-potable water demand, and the available space in the storage tanks. LCA and LCCA were then conducted to calculate life cycle cost and energy savings that can be achieved through the decentralized system installations. These savings were then optimized for each individual residential household in Boston, MA to identify the scientifically optimal locations of decentralized system installations. All models were developed using the open sourced Python 3.7. A sensitivity analysis was performed to investigate the uncertainties related to key model assumptions.

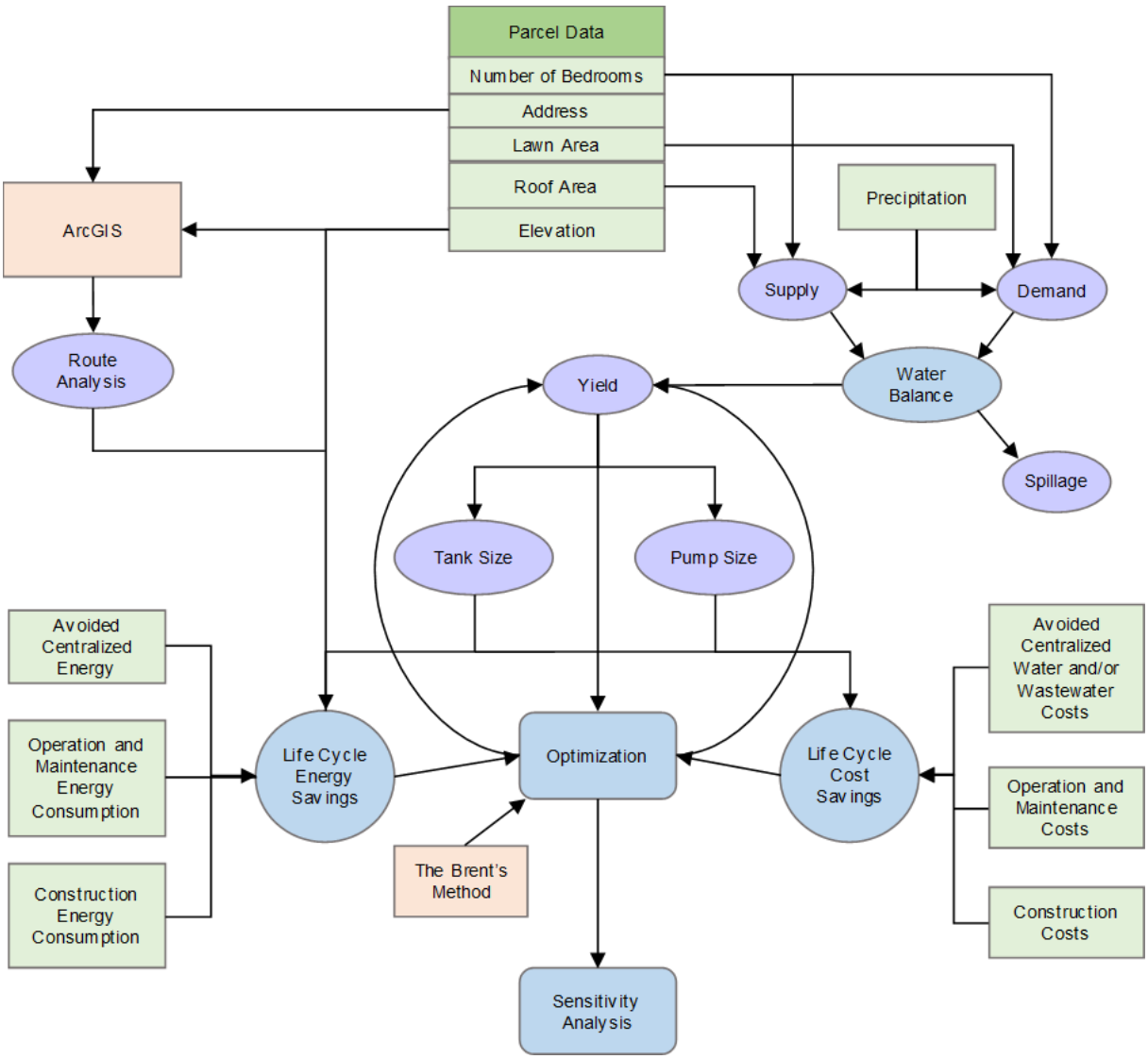

Figure 1: Rainwater and greywater modeling required the simulation of interdependent dynamic processes, including life cycles and water usage cycles.

RWH systems store rain that falls on a specific collection area. For this study, residential rooftops were the collection area for each individual system. Rainwater falls on the roof, flows by gravity to gutters, passes through a filter to remove solids, and accumulates in a storage tank at ground level (Figure 2(a)). GWR systems collect water that has already been used in a household for reuse with minimal treatment. Water from sinks, showers, and washing machines is collected in a storage tank (Figure 2(b)). Both the collected rainwater and greywater is used for non-potable uses including toilet flushing and lawn

irrigation (Dixon et al. 2000; Hamilton et al. 2017), which reduce the need for having high-quality water in the storage tank (Gwenzi et al. 2015).

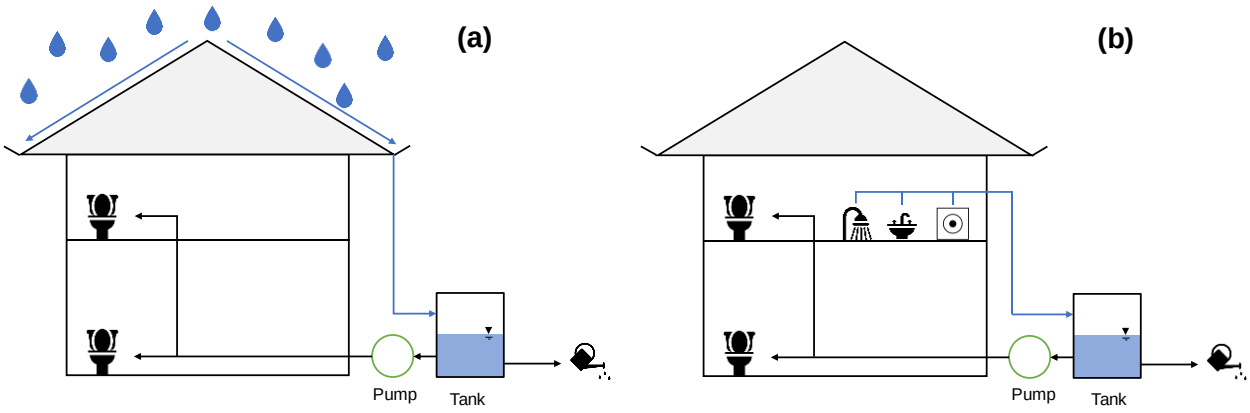

Figure 2: Rain falls on a roof, where it is collected in the gutter and diverted to the storage tank before being pumped into the household (a). Greywater is collected from various household usages, flows to the storage tank, and is pumped for toilet flushing (b).

Information for the households analyzed in the study was from the City of Boston's open-sourced GIS data portal (AB, 2019). Particularly, the 2016 tax parcel dataset has been used to obtain key attributes, including building type, street name and number, living area, number of floors, number of bedrooms, parcel square footage, average elevation, building type, and distance from the treatment plants (CB, 2019). Out of the over 160,000 property parcels included within the dataset, only residential buildings were included in the analysis. All commercial buildings as well as any buildings that did not have bathrooms and bedrooms were omitted, which reduced the data size significantly to around 68,000. Apartment units that belong to the same building were combined by matching their street addresses, which allows us to investigate decentralized system installations on a building basis.

2.2 Model Description

2.2.1 Rainwater and Greywater Supply, Yield, and Storage

The dynamic portion of the model stems from rainwater and greywater supply and demand changing daily. For both systems, the yield after spillage method was used. This algorithm has been commonly

used to simulate RWH models (Hanson et al. 2009; Wang and Zimmerman 2015). In this method, influent is collected until the storage tank has reached capacity, and the excess volume is spilled, or not collected. This excess volume becomes runoff for RWH systems or gets diverted to the sewer for GWR. Yield refers to the amount of demand that is met by the available volume in storage. When the tank is empty, the households meet their demand with potable water from their drinking water treatment plant. The dynamic equations showing the yield and storage of the tank are shown in Eqs. 1 and 2.

$$Y_t = \min \begin{cases} S_{t-1} \\ D_t \end{cases} \qquad \text{Eq. 1}$$

$$S_t = \max \begin{cases} T - Y_{t-1} \\ 0 \end{cases} \qquad \text{Eq. 2}$$

where Y_t is yield on day *t* (m³), S_{t-1} is the volume of water available in the tank from the previous day, *t-1* (m³), T is tank size (m³), and D_t is demand on day *t* (m³). Roof area was assumed to be the same as the buildings' footprint and did not include any slopes or items that may be on the roof. The National Oceanic and Atmospheric Administration's (NOAA) daily precipitation was multiplied by the roof area and a roof runoff coefficient of 0.9 to determine the total rainfall volume sent to the tank as seen in Equation 3 (Wang and Zimmerman 2015). Using NOAA's National Climate Data Center, daily precipitation data for Boston, MA was acquired from the Logan Airport gauge (NOAA 2019). Thirty years of data from 1988 to 2018 were used to simulate precipitation over the assumed 30-year life span of the decentralized systems (Morales-Pinzón et al. 2015).

$$S_{RW,t} = \min \begin{cases} RA * P_t * C_R \\ T - S_t \end{cases} \qquad \text{Eq. 3}$$

where $S_{RW,t}$ is the rainfall collected in the tank on day *t* (m³); RA is the roof area (m²); P is the amount of precipitation on day *t* (m); C_R is the roof runoff coefficient; and, S_t is the amount of water volume available in the tank on day *t* (m³).

GWR systems have a consistent daily supply dependent on occupancy (Eq. 4). Occupancy in each building was determined by the number of bedrooms within each building and the average occupancy per bedroom. The average occupancy per bedroom was calculated by dividing the total Boston population (USCB 2019) by the total number of bedrooms in the residential buildings, as obtained from the 2016 tax parcel dataset. Showers were assumed to supply 0.065 m³ per person per day; sinks were assumed to supply 0.023 m³ per person per day; and laundry supplies 0.018 m³ per person per day (USGS 2019).

$$S_{GW,t} = \min\begin{cases} N * (SH + L + SU) \\ T - S_t \end{cases} \qquad \text{Eq. 4}$$

Where $S_{GW,t}$ is the daily greywater collected in the tank (m³), N is the building occupancy, SH is the shower usage per person (m³), L is laundry demand (m³), and SU the sink usage (m³).

2.2.2 Rainwater and Greywater Demand

For this study, the non-potable uses are toilet flushing and lawn irrigation for both system types. The daily water use by toilet flushing was determined by daily flushing usage, or fixture rate, 0.072 m³ per person per day (Dieter et al. 2018), and the occupancy.

Lawn irrigation was assumed to only occur between May and September and on days when there is no precipitation (Steffen et al. 2013). On days when lawn irrigation is needed, volume was determined using Eq. 5 (Kjelgren et al. 2016).

$$D_{I,t} = \frac{E*PF*LA*a*b}{EF} \qquad \text{Eq. 5}$$

Where E is the evapotranspiration rate (in), which was assumed to be 0.06 for Boston (Romero and Duke 2014); LA is the lawn area (ft²), which was estimated by subtracting the footprint of the building from the land parcel; a is 0.62, which is the conversion of one inch of water depth to gallons per square foot of area; b is 0.0038, which is the conversion for gallons to m^3; EF is the irrigation efficiency, which was assumed to be 80% taken from a range of general lawn irrigation efficiencies (Fipps 2000); $D_{I,t}$ is irrigation demand (m^3) and PF is the plant factor, which was assumed to be 0.8 (NRCC 2019; Romero and Duke 2014).

2.3 Life Cycle Cost Model

The life cycle saving of a decentralized system depends on the capital, operation, and maintenance costs as well as the achievable economic savings over a 30-year life span. All costs were discounted back to the 2018 dollar value using an annual discount rate of 3%.

2.3.1 Capital Cost

Capital costs include construction and installation costs, while the construction cost consists of the pump cost, tank cost, and design cost. The pump cost was calculated based on the horsepower required for the household as shown in Eqs. 6 and 7 (WERF 2009). There was a minimum horsepower requirement of 0.5 due to typical pump sizes.

$$PS = \max\begin{cases} 0.5 \\ F \times NF \times W \times \frac{H}{2} / (PE \times k) \end{cases} \qquad \text{Eq. 6}$$

$$PC = \max\begin{cases} 2{,}005 \\ -31.2 * PS^2 + 486.33 * PS + 205.68 \end{cases} \qquad \text{Eq. 7}$$

where PS is pump size (hp); F is fixture rate (m^3/day); NF is number of fixtures in the building, which was estimated to be occupancy divided by 1.5; g is gravity, or 9.81 m/s^2; k is the conversion of joules to kWh or 3.6 * 10^6; $W$is the water density (kg/ m^3); H is building height (m); PC is pump cost ($); and PE is pump efficiency, which was assumed to be 0.8.

The tank cost was a function of tank size (Eq. 8;(WERF 2009)). Tanks were assumed to be made of plastic materials.

$$TC = 358.77 * (T^{0.5064}) \qquad \text{Eq. 8}$$

Where TC is tank cost ($) and T is tank size (m^3).

Installation cost is the cost of implementing the system in the home and was assumed to be 60% of the tank cost (WERF 2009), while the design cost was assumed to be 8% of the sum of the capital costs and maintenance cost (WERF 2009).

2.3.2 Operation and Maintenance Cost

The operation cost was calculated based on the pumping energy for operating the decentralized systems. The system's pumping energy demand is dependent on the home's indoor use ratio. Indoor use ratio refers to the proportion of rainwater or greywater that was used for toilet flushing out of the total yield on a particular day. We assumed only the water for toilet flushing needs to be pumped upwards, and irrigation was assumed to be gravity-fed. The height for water lifting was assumed to be half of the building height. The daily pumping energy was calculated using Eq. 9.

$$PEC_t = Y_t * IU_t * W * g * \left(\frac{H}{2}\right) * \frac{j}{PE_D} * EP \qquad \text{Eq. 9}$$

where PEC_t is pumping energy cost on day t (\$); Y_t is yield on day t (m^3); W is water density (kg/m^3); j is the conversion from kWh to joules, which is 2.78 * 10^{-7}; IU_t is indoor use ratio on day t; H is building height (m); PE_D is pump efficiency, which was assumed to be 0.5; and EP is the electricity price (\$/kWh), which was assumed to be \$0.216/kWh for Boston (BLS 2019).

Maintenance cost was set at \$100 annually, which falls within the suggested range by various literature sources (WERF 2009; USEPA 2013). Maintenance of the system is required to ensure the tank and filter are in proper working order and unobstructed by clogs or failing equipment.

2.3.3 Cost Benefit

RWH systems prevent owners from needing to purchase potable water from the centralized drinking water plant. GWR systems prevent owners from needing to purchase potable water as well as from sending the greywater to the sewer. Both benefits reduce the customer's monthly water bills. Boston's 2018 water rates were used for the simulation, with \$1.82 per m^3 for purchased potable water and \$2.41 per m^3 for sewer (BWSC 2019). For GWR systems, the combined savings per reused unit of greywater was \$4.23 per m^3. It is typical that a sewer meter is not installed in addition to the potable water meter, and the wastewater quantity is assumed to be the same as the amount of drinking water used. However, landlords in Massachusetts are permitted to implement individual sewer meters in each unit to accurately measure sewerage. For this reason, the model for the GWR system reflects the reduced sewer flow and subsequent utility bill savings.

2.4 Life Cycle Energy Model

The life cycle energy model considers the energy expenditure of installing and operating a RWH or GWR system and the avoided energy for pumping and treatment at the centralized water and wastewater treatment plants. Particularly, RWH systems affect the pumping and treatment energy use in the drinking

water plant, while the GWR systems affect the energy use in both the drinking water and the wastewater treatment plants.

2.4.1 Avoided Pumping Energy

The avoided pumping energy from the centralized treatment plants was estimated based upon four components: friction head loss, elevation head, operating head, and velocity head using Eqs. 10-13. While all four components were considered for the avoided pumping energy from the centralized drinking water plant, only friction head loss and elevation head were considered for the centralized wastewater treatment plant.

$$PM = \frac{OF * W * g * (FL + \Delta E + OP + VH)}{CP * k} \quad \text{Eq. 10}$$

$$FL = FC * DP \quad \text{Eq. 11}$$

$$\Delta E = \begin{cases} HE - PE & if \quad HE - PE > 0 \\ 0 & if \quad HE - PE < 0 \end{cases} \quad \text{Eq. 12}$$

$$VH = 0.5 * V^2/g \quad \text{Eq. 13}$$

where PM is centralized pumping energy savings (kWh); OF is the outflow of the pumps, which was assumed to be equal to the rainwater or greywater yield for each household (m^3); W is the water density, 1,000 kg/m^3; CP is the pumping efficiency of the centralized pumps, which was assumed to be 50%; TH is total head (m); FL is friction loss (m); ΔE is the elevation head (m); OP is operating head of the centralized pumps (m), which was assumed to be only applicable to drinking water system; VH is the velocity head or the dynamic pressure (m), which was assumed to be only applicable to drinking water system; FC is friction loss coefficient (m/km); DP is distance between the household and the treatment

plant (km); HE is household elevation (m), PE is plant elevation (m); and V is water velocity in the pipe (m/s).

To find the friction water head, the minimum piping distance from each building to the drinking water plant, the John J. Carroll Water Treatment Plant, and the wastewater treatment plant, the Deer Island Sewage Treatment Plant, need to be determined. Boston's road network was used to estimate the piping distances, assuming water and wastewater pipes were located along the roads (Kavvada et al. 2016). A road network dataset was collected from the Boston's GIS data portal (AB; Analyze Boston 2019; CB; City of Boston 2019). Approximate piping distance between the households and the plants was found using the Network Analyst toolset in ArcMap 10.6, using the closest facility function. The network was completed by finding the centroid of each parcel, determining the closest road to each centroid, and creating a line from the centroid to the road network. The coordinates for the John J. Carroll Water Treatment Plant and the Deer Island Sewage Treatment Plant were obtained from Google Earth and added to the road network layer using the geo-referencing tool in ArcMap. The residential buildings and their corresponding data were placed in the road network layer using address locators to ensure correct coordinates to find the distance to the water and wastewater treatment plants. The friction loss coefficient was estimated to be 8 m/km, based on approximate pipe material and diameter (Ghorbanian, Karney, and Guo 2016; NRCNA 2006). Elevation head was determined using an elevation contours dataset from Boston's GIS data portal (AB 2019). The elevation of each parcel was determined by finding the average elevation spatially across the parcel to calculate elevation head. Operating head at the plant was assumed be 70 psi to meet 27.5 psi at the withdrawal point, which is recommended for water distribution systems to meet maximum daily demand and fire flow conditions.

An empirical method was used to calibrate the modeled pumping energy to ensure that it does not exceed the total pumping energy used by the plants. To achieve this, annual total operational energy usages were obtained from the John J. Carroll Water Treatment Plant and the Deer Island Sewage Treatment Plant,

which are 0.22 MJ/m^3 and 2.14 MJ/m^3, respectively. As the amounts of pumping energy usages were not directly available to the authors, we assumed pumping represents 86% of the drinking water plant's operational energy (EPRI 2002) and 14% of the wastewater treatment plant's operational energy. Based upon these percentages, the pumping energy intensity was estimated to be around 0.19 MJ/m^3 for the John J. Carroll Water Treatment Plant and 0.30 MJ/m^3 for the Deer Island Sewage Treatment Plant. Modelled unit pumping energy savings from the centralized drinking water and wastewater treatment plants were calculated by summing up the avoided drinking or wastewater pumping energy from all households in the dataset over the 30-year life cycle and divide it by the total yield from all households over 30 years. The modelled pumping energy intensities were then adjusted to match the real ones. A correction factor of 0.92 and 0.89 was applied to the modelled avoided pumping energy from the centralized drinking water and wastewater treatment plants, respectively.

The calibrated pumping energy was then converted to the primary energy form for estimation of life cycle energy. A conversion factor of 1.5 MJ/MJ was obtained from SimaPro 8.5 by applying the *Cumulative Energy Demand V1.10* method to a data entry named "*Electricity, medium voltage {US}| market group for | Conseq, U*".

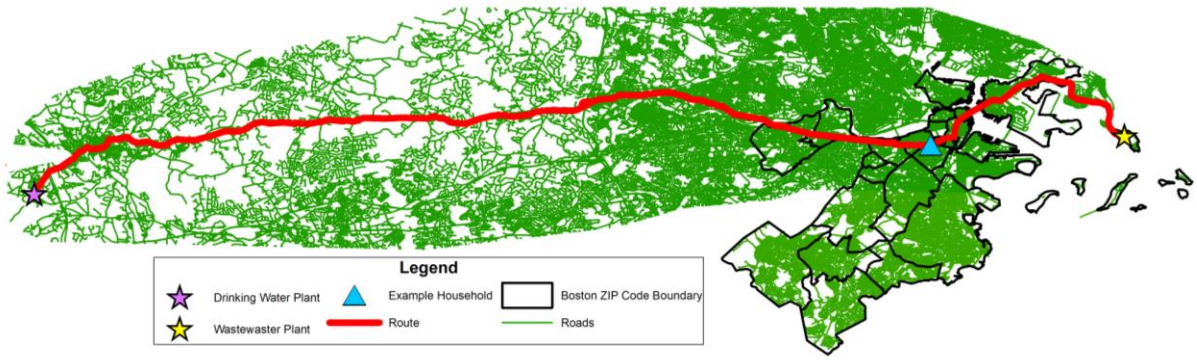

Figure 3: The water's path from the drinking water plant, to the households in Boston, and then to the wastewater plant was mapped via Massachusetts's road network, which was assumed to reflect the placement of distribution and collection pipes.

2.4.2 Avoided Treatment Energy

The avoided treatment energy was obtained from previous life cycle assessment studies on the John J. Carroll Water Treatment Plant and the Deer Island Wastewater Treatment Plant. The energy intensity of drinking water treatment was assumed to be 1.13 62 MJ/m^3 of primary energy, while the energy intensity of wastewater treatment was assumed to be 1.68 MJ/m^3 of primary energy.

2.4.3 Energy Used for Constructing, Operating, and Maintaining Decentralized Systems

Construction energy is a single energy expenditure that accounts for pump manufacturing, tank manufacturing, and installation. These three components were calculated using the Economic Input-Output Life Cycle Assessment (EIOLCA) web tool (Carnegie Mellon University 2018). The pump and pumping equipment manufacturing sector was used for the pump manufacturing energy intensity, and the associated embodied energy intensity was 8.49 MJ of primary energy/dollar. The total pump manufacturing energy was estimated as a product of the estimated pump cost (Eq. 7) and the pump manufacturing energy intensity. The other plastic products manufacturing sector was used for tank manufacturing, and the embodied energy intensity was 14.8 MJ of primary energy/dollar. The total tank manufacturing energy was a product of the estimated tank cost (Eq. 8) and the tank manufacturing energy intensity. The residential permanent site single- and multi-family structures sector was used to find the energy intensity of installation, and its embodied energy intensity was 6.21 MJ of primary energy/dollar. Similarly, the total installation energy was estimated as a product of installation cost and the installation energy intensity. The operation energy usages of the decentralized systems were calculated as a part of Eq. 9. The calculated pumping energy was converted to the primary energy form using a factor of 5.4 MJ/kWh. The maintenance energy of the decentralized systems was calculated using the EIO-LCA tool. The other support services sector was used to find the energy intensity of maintenance, which was 3.58 MJ/dollar (Carnegie Mellon University 2018). The total maintenance energy was estimated as a product of maintenance cost and the maintenance energy intensity. Energy usage for the decentralized system was calculated for each of the residential households in the Boston tax parcel dataset.

2.5 Optimization of Tank Sizes

Tank size was optimized for each household to maximize either net cost or energy savings. The Brent's method was used to select the optimal tank size. The Brent's method searches for the maximum savings point of each household using the bisection method, secant method, and inverse quadratic interpolation. The bisection method splits the output data in half until it finds the point of interest, in this case the maximum cost or energy savings. To use the Brent's method, scipy.optimize and negative minimized scalar function was coded, with an accuracy range of 0.2 m^3. Since the Brent's method requires bounds to operate within, the maximum possible tank size was determined to be 40 m^3. Brent's method assumes the function is concave. If the model's output does not result in a concave function, the maximums selected may not be unique. However, in our model tests on randomly selected households, we found all of the cost and energy results as a function of tank size are concave. Two optimal sizes were selected for each system, one based on the highest cost savings and one based on the highest energy savings (or lowest energy losses). The two optimal tank sizes were not dependent on each other and could vary greatly.

2.6 Sensitivity Analysis

To evaluate which variables had the greatest effect on the system dynamics outcomes for cost and energy, a sensitivity analysis was conducted. Analyses were performed for RWH energy savings, RWH cost savings, GWR energy savings, and GWR cost savings. The attributes varied and tested were height per floor, electricity price, pump efficiency, water price, fixture rate, lawn condition, irrigation efficiency, water velocity in pipes, discount rate, laundry loads, shower flow, sink flow, evapotranspiration rate, and plant factor. Input variables were changed by ±25% and ±50% to represent a reasonable range of possible values. To determine the variables' influence on the outcomes, Equation 11 was used to create a sensitivity index. Variables were considered highly sensitive if their indices were greater than one.

$$SI = \frac{\frac{CO - OO}{OO}}{\frac{CI - OI}{OI}} \quad \text{Eq. 11}$$

where SI is sensitivity index, CO is the changed output value, OO is the original output value, CI is changed input value, and OI is original input.

3. Results and Discussion

3.1 Spatial Distribution of RWH and GWR Savings in Boston

Figure 4 presents the net life cycle cost and energy savings of RWH for each of the residential household in Boston. According to our analysis, no optimized RWH systems would provide energy savings and few RWH systems could offer cost savings. All the systems would cause an overall increase in embodied energy usage for water supply, largely due to the energy intensity associated with constructing and implementing the system. The average net energy consumption was 1,128 MJ/year with an averaged optimal tank size of 0.3 m^3 if every household adopts a RWH system, and the average net cost was \$107/year with an averaged optimal tank size of 3.9 m^3. The pumping and treatment energy savings at the drinking water plant were found to never be greater than the embodied energy associated with adopting a RWH system in a 30-year time frame. The energy model selected the tank size closest to zero to minimize the overall energy loss.

Out of the nearly 70,000 buildings that were optimized, about 350 of them had cost savings. These savings ranged from \$0.03-200/year. Households that resulted in cost savings had one of two characteristics: 30 or more bedrooms, or a lawn size that was at least double the size of the building's footprint.

The buildings that benefited from cost savings also have tank sizes of 8 m^3 or greater.
Buildings with more bedrooms have more tenants and therefore have a higher demand.
The water demand of buildings with small roof sizes and large lawns may often exceed the supply available from their tanks, so their RWH system will be heavily relied upon for irrigation.

Most of the buildings that had cost savings were located in downtown Boston, where there are more large residential buildings with higher occupancies. Figure 4 shows the energy and cost savings distribution of RWH systems over 30 years in Boston.

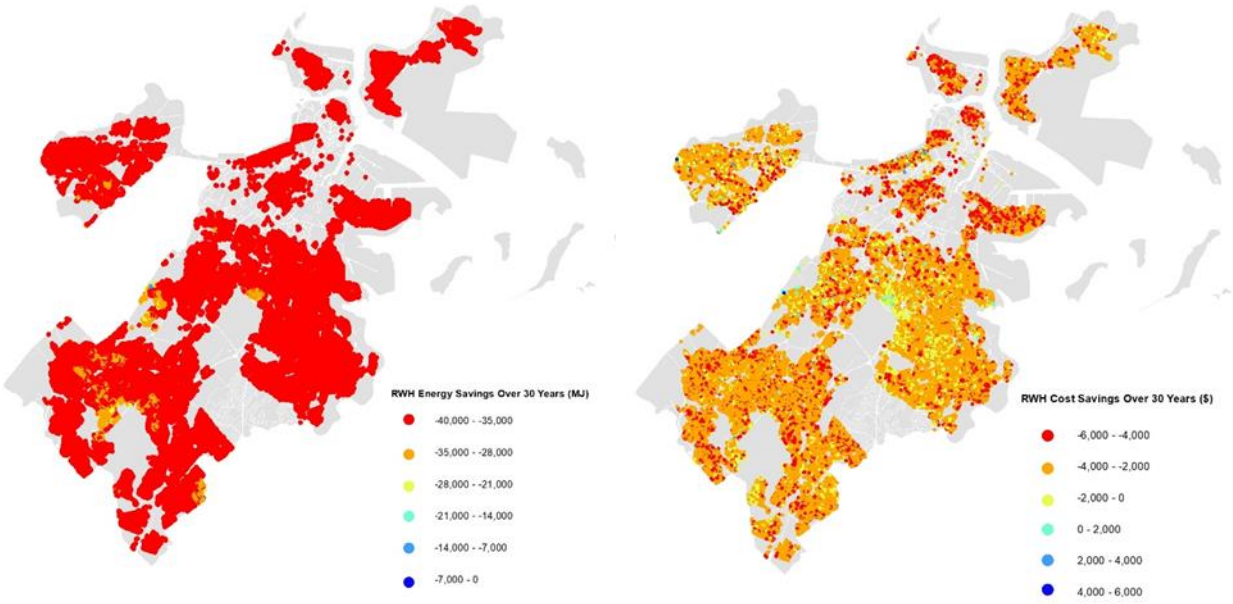

Figure 4: All RWH energy savings throughout Boston were negative after 30 years, shown on the left. Most RWH cost savings were negative with a few households in central Boston experiencing positive savings, shown on the right.

Over 95% of the households that were modelled had energy and cost savings from GWR systems. GWR are beneficial because they offer cost and energy savings through wastewater diversion, which is an energy intensive and expensive process. The average energy savings was -5,169 MJ with an optimal tank size of 1.3 m^3, and the average cost savings was $26,510 with a tank size of 11.2 m^3. Households with the highest number of tenants and the largest lawn size compared to the roof area had the highest cost and energy savings. Larger systems could offer economies of scale due to a higher water cost savings to construction cost ratio. GWR has a constant daily supply for water use due to the approximated daily water use per person. Boston's Back Bay area had the largest occurrence of buildings with high cost and

energy savings compared to the rest of the city. Figure 5 shows the spatial distribution of cost and energy savings for GWR systems in the Boston metro area.

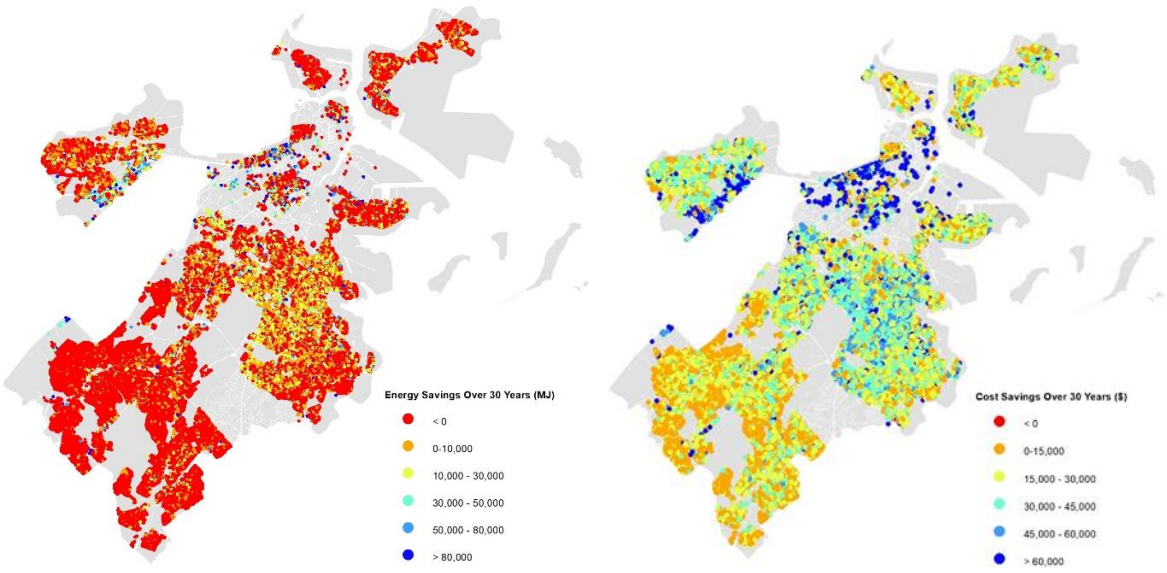

Figure 5: GWR energy savings were mostly negative at the edges of Boston, while the center of Boston and downtown Boston experienced positive savings. Every household resulted in cost savings for GWR, with downtown Boston having the largest savings after 30 years.

Overall, GWR systems offered greater cost and energy savings throughout Boston if adopted. This could be because GWR systems have a constant daily supply of water available for recycling while RWH systems have varying daily supplies. On both GWR maps and the RWH energy map, there is an area in the northwest center where there is a large concentration of high savings. This area, known as Back Bay, has one of the highest population densities in Boston and has a high average household income (BPDA; Boston Planning & Development Agency 2019). The high population density in this area can be attributed to the closely grouped apartments with four to six floors that largely make up Back Bay. Back Bay's buildings on average are some of the oldest in the city (NTHP; National Trust for Historic Preservation 2019). Old buildings may be the ones most likely to be renovated for updates, and they could more easily be retrofitted for decentralized systems during this process. Meanwhile, households in Back Bay have a relatively higher affordability of the initial cost of the decentralized systems. Most of the

households in Hyde Park, an area in south Boston, cannot benefit from installations of decentralized water systems from both energy and cost perspectives. This area has a low average income, low population density, a mix of new and old buildings, as well as a relatively lower affordability of the initial costs of the decentralized systems. Maintaining affordable and reliable centralized water service to the area is hence critical. This also indicates the need of further lowering the cost and energy intensity of decentralized systems to increase its competitiveness as an alternative water source.

3.2 Sensitivity Analysis

The GWR energy and RWH energy models did not have any highly sensitive variables. GWR cost was highly sensitive to floor height with a sensitivity index of 1.5. Floor height determined the height that the households' pump would have to deliver the collected water from the tank to the point of use. The higher the water had to travel, the more energy the pump would use, which is an increase in electricity costs for the household. RWH cost was sensitive to water price with a peak sensitive index of 1.1. The lower the water price, the less savings a household can incur per unit of water. Figure 6 shows the sensitivity indices for the cost model.

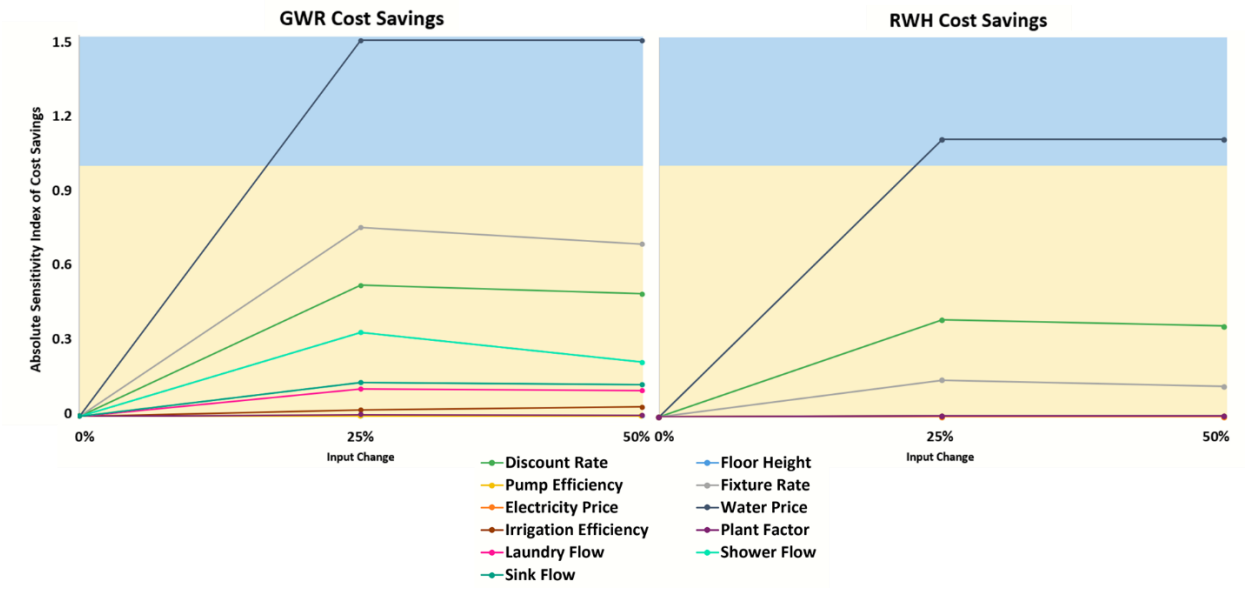

Figure 6: Water price was determined to have a significant absolute sensitivity (greater than 1) for both cost savings models, shown in the blue section of the graphs.

4. Conclusion

This study used a Python model to optimize the tank sizes of GWR and RWH decentralized systems for households in Boston based on cost savings to the homeowners and energy savings for the water distribution system.

Two system dynamics models, one for RWH and one for GWR, were first developed to simulate the daily water balance based upon the supply of rainwater or greywater, the non-potable water demand, and the available space in the storage tanks. LCA and LCCA were then conducted to calculate life cycle cost and energy savings that can be achieved through the decentralized system installations. These savings were then optimized for each individual residential household in Boston, MA to identify the scientifically optimal locations of decentralized system installations.

The results showed that RWH systems rarely offered cost savings for homeowners, and very few RWH systems could provide energy savings after 30 years. GWR systems were more likely to benefit

households for cost and energy savings, with applicable households throughout the Boston metro area. An area of large, old buildings in Boston had the highest potential cost and energy savings if a GWR system was adopted.

A changing economy or environment could also impact the economic and energy feasibility of GWR and RWH. If the utility prices of water and wastewater increase, homeowners could potentially see higher cost savings with the use of water that is recycled or reused. Water and wastewater treatment could also become more require more energy, as emerging pollutants are regulated and new, energy-intensive steps need to be added to the treatment train. GWR and RWH systems could reduce the volume of water required to go through more rigorous treatment. Climate change could also play a role in the importance of decentralized adoption. Other areas around the country are expected to see reduced rainfall and increased evaporation, placing stress on surface water withdrawals for drinking water. GWR and RWH systems could alleviate some of the stress on the system by sourcing water from other areas.

For holistic infrastructure planning, a policy could be put in place to add a decentralized system when older buildings are renovated if they could benefit. For low income areas that cannot benefit from decentralized water systems due to their household characteristics, a subsidy could be given to offset their water bills. This model can be applied to any region to assist with decision making for water distribution management.

RWH has been accepted worldwide as a source of water for non-potable uses for generations, particularly for irrigation (USEPA, 2013). Conversely, GWR has had low public support (Oteng-Peprah et al., 2018). This could be due to misinformation surrounding greywater, dislike of the idea of used water being close to human contact, and push back against new technology (Oteng-Peprah et al., 2018). To encourage adoption of GWR, city planners could develop an education and outreach plan to inform homeowners and developers about the environmental and economic benefits of GWR and its low health risk.

REFERENCES

AB; Analyze Boston. 2019. “Analyze Boston.” https://data.boston.gov/.

Ángel, Miguel et al. 2016. “Potential of Rainwater Harvesting and Greywater Wastewater Minimization.” : 1–18.

Angrill, Sara et al. 2012. “Environmental Analysis of Rainwater Harvesting Infrastructures in Diffuse and Compact Urban Models of Mediterranean Climate.” : 25–42.

ASCE; American Society of Civil Engineers. 2017. “Water Infrastructure | ASCE’s 2017 Infrastructure Report Card.” *American Society of Civil Engineers*. https://www.infrastructurereportcard.org/cat-item/drinking-water/.

AWWA; American Water Works Association. 2001. “Dawn of the Replacement Era - Reinvesting in Drinking Water Infrastructure.” *AWWA* 80235(303).

BLS; Bureau of Labor Statistics. 2019. “Average Energy Prices in Boston-Cambridge-Newton.” https://www.bls.gov/regions/new-england/news-release/averageenergyprices_boston.htm.

Bowen, J. L. et al. 2019. “Boston Harbor, Boston, Massachusetts, USA: Transformation from ‘the Harbor of Shame’ to a Vibrant Coastal Resource.” *Regional Studies in Marine Science*.

BPDA; Boston Planning & Development Agency. 2019. “U.S. Census and Demographics Maps.” http://www.bostonplans.org/3d-data-maps/gis-maps/census-and-demographic-maps.

BWSC; Boston Water and Sewer Commission. 2019. “Boston Water and Sewer Rates.” https://www.bwsc.org/residential-customers/rates.

Carnegie Mellon University. 2018. “Economic Input-Output Life Cycle Assessment.” http://www.eiolca.net/.

CB; City of Boston. 2019. “BostonMaps Open Data Geospatial Datasets.” http://bostonopendata-boston.opendata.arcgis.com.

Chang, Jin, Woojin Lee, and Sukhwan Yoon. 2017. “Energy Consumptions and Associated Greenhouse Gas Emissions in Operation Phases of Urban Water Reuse Systems in Korea.” *Journal of Cleaner Production*.

Dieter, Cheryl A. et al. 2018. *Estimated Use of Water in the United States in 2015: U.S. Geological Survey Circular 1441*.

Dixon, A, D Butler, A Fewkes, and M Robinson. 2000. “Measurement and Modelling of Quality Changes in Stored Untreated Grey Water.” 1(1999).

EPRI. 2002. 4 Water Supply *Water & Sustainability (Volume 4): U.S. Electricity Consumption for Water Supply & Treatment - The Next Half Century*. Palo Alto, CA.

Fipps, Guy. 2000. “Calculating Horsepower Requirements and Sizing Irrigation Supply Pipelines.”

Ghimire, Santosh R, John M Johnston, Wesley W Ingwersen, and Troy R Hawkins. 2014. “Life Cycle Assessment of Domestic and Agricultural Rainwater Harvesting Systems.”

Ghisi, Enedir, Ricardo Forgiarini Rupp, and Yuri Triska. 2014. “Comparing Indicators to Rank Strategies to Save Potable Water in Buildings.” *Resources, Conservation and Recycling* 87: 137–44.

Ghorbanian, Vali, Bryan Karney, and Yiping Guo. 2016. “Pressure Standards in Water Distribution Systems: Reflection on Current Practice with Consideration of Some Unresolved Issues.” *Journal of Water Resources Planning and Management* 142(8): 04016023.

Godskesen, B. et al. 2011. “Life Cycle Assessment of Three Water Systems in Copenhagen-a Management Tool of the Future.” *Water Science and Technology* 63(3): 565–72.

Godskesen, B et al. 2013. “Life-Cycle and Freshwater Withdrawal Impact Assessment of Water Supply Technologies.” 7.

Gwenzi, Willis et al. 2015. “Water Quality and Public Health Risks Associated with Roof Rainwater Harvesting Systems for Potable Supply: Review and Perspectives.” *Sustainability of Water Quality and Ecology*.

Hamilton, Kerry A., Warish Ahmed, Simon Toze, and Charles N. Haas. 2017. “Human Health Risks for Legionella and Mycobacterium Avium Complex (MAC) from Potable and Non-Potable Uses of Roof-Harvested Rainwater.” *Water Research*.

Hanson, Lars S, Richard M Vogel, Paul Kirshen, and Peter Shanahan. 2009. “Generalized Storage-Reliability-Yield Equations for Rainwater Harvesting Systems.” *Proceedings of World Environmental and Water Resources Congress 2009* 342: 115. http://link.aip.org/link/?ASC/342/115/1.

Hargreaves, Anthony J, Raziyeh Farmani, Sarah Ward, and David Butler. 2019. “Modelling the Future Impacts of Urban Spatial Planning on the Viability of Alternative Water Supply.” *Water Research* 162: 200–213. https://doi.org/10.1016/j.watres.2019.06.029.

Hunter, Paul R, Alan M Macdonald, and Richard C Carter. 2010. “Water Supply and Health.” *PLoS Medicine* 7(11).

Jeong, Hyunju et al. 2016. “Life Cycle Assessment of Low Impact Development Technologies Combined with Conventional Centralized Water Systems for the City of Atlanta, Georgia.” *Frontiers of Environmental Science and Engineering* 10(6): 1–13.

JFW; The Johnson Foundation at Wingspread. 2014. “Integrating Distributed Systems.” (August).

Kavvada, Olga et al. 2016. “Assessing Location and Scale of Urban Nonpotable Water Reuse Systems for Life-Cycle Energy Consumption and Greenhouse Gas Emissions.” *Environmental Science and Technology* 50(24): 13184–94.

Kjelgren, R., R. C. Beeson, D. R. Pittenger, and D. T. Montague. 2016. “Simplified Landscape Irrigation Demand Estimation: Slide Rules.” *Applied Engineering in Agriculture* 32(4): 363–78.

Matteo, Michael Di, Graeme C. Dandy, and Holger R. Maier. 2017. “Multiobjective Optimization of Distributed Stormwater Harvesting Systems.” *Journal of Water Resources Planning and Management* 143(6): 04017010.

Memon, F. A. et al. 2007. “Life Cycle Impact Assessment of Greywater Recycling Technologies for New Developments.” *Environmental Monitoring and Assessment* 129(1–3): 27–35.

Morales-Pinzón, Tito, Joan Rieradevall, Carles M. Gasol, and Xavier Gabarrell. 2015. “Modelling for Economic Cost and Environmental Analysis of Rainwater Harvesting Systems.” *Journal of Cleaner Production* 87(1): 613–26.

Newman, J P, G C Dandy, and H R Maier. 2015. “Multiobjective Optimization of Cluster-Scale Urban Water Systems Investigating Alternative Water Sources and Level of Decentralization.” *Water Resources Research* 50(December 2009): 7915–38.

NOAA; National Oceanic and Atmostpheric Association. 2019. “National Centers for Environmental Information: Climate Data Online.” https://www.ncdc.noaa.gov/cdo-web/.

NRCC. 2019. “Monthly Average Potential Evapotranspiration (PET) Estimates (Inches).”

NRCNA; National Research Council of the National Academies. 2006. *Drinking Water Distribution Systems: Assessing and Reducing Risk*. https://www.nap.edu/read/11728/chapter/1.

NTHP; National Trust for Historic Preservation. 2019. “The Atlas of ReUrbanism.” https://forum.savingplaces.org/act/research-policy-lab/atlas/map.

Oteng-Peprah, Michael, Mike Agbesi Acheampong, and Nanne K. DeVries. 2018. “Greywater Characteristics , Treatment Systems , Reuse Strategies and User Perception — a Review.” *Water, Air, and Soil Pollution*.

Penn, Roni, Eran Friedler, and Avi Ostfeld. 2013. “Multi-Objective Evolutionary Optimization for Greywater Reuse in Municipal Sewer Systems.” *Water Research*.

Romero, Consuelo C, and Michael D Duke. 2014. “Turfgrass Crop Coefficients in the U . S .” (May).

Steffen, Jennifer, Mark Jensen, Christine A. Pomeroy, and Steven J. Burian. 2013. “Water Supply and Stormwater Management Benefits of Residential Rainwater Harvesting in U.S. Cities.” *Journal of the American Water Resources Association* 49(4): 810–24.

USCB; U.S. Census Bureau. 2019. “American Fact Finder.” https://factfinder.census.gov/faces/nav/jsf/pages/index.xhtml.

USEPA; United States Environmental Protection Agency. 2013. “Rainwater Harvesting: Conservation, Credit, Codes, and Cost.” (January): 41p.

USGS; United States Geological Survey; U.S. Department of the Interior. 2019. “USGS Domestic Water Use.” https://www.usgs.gov/mission-areas/water-resources/science/domestic-water-use?qt-

science_center_objects=0#qt-science_center_objects.
Wang, Ranran, and Julie B. Zimmerman. 2015. “Economic and Environmental Assessment of Office Building Rainwater Harvesting Systems in Various U.S. Cities.” *Environmental Science and Technology* 49(3): 1768–78.
Wanjiru, Evan, and Xiaohua Xia. 2017. “Optimal Energy-Water Management in Urban Residential Buildings through Grey Water Recycling.” *Sustainable Cities and Society* 32(October 2016): 654–68. https://doi.org/10.1016/j.scs.2017.05.009.
Ward, S, F A Memon, and D Butler. 2012. “Performance of a Large Building Rainwater Harvesting System.” *WR* 46(16): 5127–34. http://dx.doi.org/10.1016/j.watres.2012.06.043.
WERF; The Water Research Foundation. 2009. “The Water Research Foundation.” https://www.werf.org/.